

# Witnessing mass-energy equivalence with trapped atom interferometers

Jerzy Paczos,<sup>1,\*</sup> Joshua Foo,<sup>2,3,†</sup> and Magdalena Zych<sup>1,4,‡</sup>

<sup>1</sup>*Department of Physics, Stockholm University, SE-106 91 Stockholm, Sweden*

<sup>2</sup>*Centre for Quantum Computation and Communication Technology,  
School of Mathematics and Physics, University of Queensland, St. Lucia, Queensland 4072, Australia*

<sup>3</sup>*Department of Physics, Stevens Institute of Technology,  
Castle Point Terrace, Hoboken, New Jersey 07030, USA*

<sup>4</sup>*Centre for Engineered Quantum Systems, School of Mathematics and Physics,  
The University of Queensland, St. Lucia, Queensland, 4072, Australia*

(Dated: September 24, 2024)

We propose an experimental setup to probe the interplay between the quantum superposition principle and the gravitational time dilation arising from the mass-energy equivalence. It capitalizes on state-of-the-art atom interferometers that can keep atoms trapped in a superposition of heights in Earth’s gravitational field for exceedingly long times reaching minute-scale. Our proposal consists of adding two additional laser pulses to the existing setups that would set up a clock trapped at a superposition of heights reading a quantum superposition of relativistic proper times. We develop a method to include relativistic corrections to Bloch oscillations which describe the trapped part of the interferometer. As a result, we derive all the trajectories arising in this setup, the phases acquired by different trajectories in the interferometer, and demonstrate that the effect of superposition of proper times would manifest itself in the interference pattern in two distinct ways: as visibility modulations, and as a shift of the resonant frequency of the atom. We argue that the latter might be observable with current technology.

—*Introduction.* A key prediction of general relativity is that time is not a global background parameter but flows at different rates depending on the spacetime geometry, a phenomenon known as time dilation [1]. The physical effects produced by time dilation have been tested in numerous paradigmatic experiments. Pound and Rebka were the first to observe an altitude-dependent gravitational redshift in gamma rays emitted between the top and bottom of a tower [2]; Hafele and Keating directly tested special and general relativistic time dilation by comparing actual clocks at different heights and moving at different speeds [3]; while Shapiro proposed to measure the reduction of the speed of light for electromagnetic waves traveling across regions subject to a gravitational potential [4], which was observed in [5]. The above effects are fully explainable within the paradigm of classical (non-quantum) relativistic physics.

The first experiment measuring the effect of gravity on the quantum wavefunction of a single particle was performed by Colella, Overhauser, and Werner (COW) [6]. The setup considered neutrons traveling in a superposition of heights in the Earth’s gravitational field, following the basic geometry of a Mach-Zehnder-type interferometer. The neutrons, traversing arms at different heights in the gravitational potential acquire a relative phase. The resulting interference pattern was measured and a phase difference consistent with the Earth’s gravitational potential was deduced. These and related effects measured with atoms [7–22] are thus tests of the non-relativistic

gravitational effects in quantum systems.

Hence, none of the experiments performed so far probe the interplay between quantum mechanics and general relativity — the idea of how to do it was only developed in [23, 24]. These works considered interferometric experiments with a particle having an internal degree of freedom that could be treated operationally as a “quantum clock”. The internal evolution would then depend on the proper time along the paths taken through general curved spacetime [23–34]. Specifically, the authors of [24] predicted that in the proposed experiment one would observe oscillations of the visibility of the interference pattern, defined as the contrast between the constructive and destructive interference fringes (which in the non-relativistic theory in the COW-type experiments is, in principle, always maximal). The predicted periodic modulations of the visibility would be an effect that arises unambiguously from the interplay between relativistic and quantum physics. Several proposals were made to probe this effect in interferometric experiments with electrons [35] and atoms [27, 28, 36–38]. However, given the size of the interferometer required for a reasonable visibility drop [24] it is rather unlikely that this effect will be observed anytime soon.

Derivations of the dynamics of relativistic quantum particles with quantized internal mass-energy, necessary to make predictions for the above experiments, have been done in the framework of relativistic quantum mechanics in refs [39–42], and starting from quantum field theory in curved background in refs [28, 43, 44]. In the low energy limit for the center of mass of the composite particles, they coincide. These results were applied to modeling the dynamics of particles in clock interferometers [27, 28, 35–37, 45] and of trapped particles [46], in particular in the

\* [jerzy.paczos@fysik.su.se](mailto:jerzy.paczos@fysik.su.se)

† [jfoo@stevens.edu](mailto:jfoo@stevens.edu)

‡ [magdalena.zych@fysik.su.se](mailto:magdalena.zych@fysik.su.se)

context of optical clocks to explore relativistic contributions to the clock's frequency and precision in refs [47–49], and most recently to explore associated many-body effects [50].

In this work, we propose a concrete experimental setup for witnessing time dilation effects in atom interference. Our idea is inspired by the rapid development of trapped atom interferometers [18–22] utilizing Bloch oscillations to keep atoms in a coherent superposition of heights in a gravitational field for increasingly long times, reaching minute-scale [22]. We propose a modification of the existing interferometers in the form of two additional “clock pulses” at the beginning and the end of the Bloch oscillations. This procedure effectively sets up a clock at a superposition of heights in the gravitational field, which means that the clock experiences a superposition of proper times. We develop a method to account for relativistic mass-energy corrections in Bloch oscillations and use it to derive all the phases acquired by different trajectories within the interferometer and analyze the interference pattern. We recover the visibility modulations predicted in [24], where fixed classical trajectories of the clocks within the interferometer were assumed, but crucially, we predict the clock's frequency shift, making this proposal feasible.

Indeed, the proposed setup implements Ramsey spectroscopy for spatially superposed atoms, allowing for measurements of their resonant frequencies. We show that relativistic effects manifest therein as resonant-frequency shifts. We argue that this will be easier to observe than the visibility oscillations due to the enormous precision of frequency measurements [51, 52]. In particular, for the height separations reported in ref. [20], the predicted fractional frequency shift is of the order of  $10^{-22}$ , one order of magnitude below the current measurement precision. Revealing effects potentially detectable with current technology, our proposal constitutes a major step toward experimental tests of the interplay between quantum mechanics and general relativity. —*Setup.* Let us consider a one-dimensional atom interferometry setup, Fig. 1, closely resembling configurations implemented in [18–22]. It involves a highly cooled atom [53] moving along the gravitational field  $g$  with velocity modified by Bragg pulses and an optical lattice. We assume a two-level internal structure of the atom with the ground and excited states separated by energy  $\hbar\omega_0$ .

First, atoms are prepared in the ground state and launched upwards into free fall with initial velocity  $v_0$ . Next, a pair of  $\pi/2$  Bragg pulses are applied separated by a time  $T$ . Each of them splits the atomic trajectory into two — one with unchanged velocity, and one with velocity modified by  $\Delta v$ . Therefore, after this sequence, the initial trajectory of each atom is split into four paths with pairwise equal velocities — one pair with velocity  $v_0 - gT$ , and the other pair with velocity greater by  $\Delta v$ . We focus on the latter pair and assume that the track of the remaining trajectories is lost as in experiments in refs [18–22].

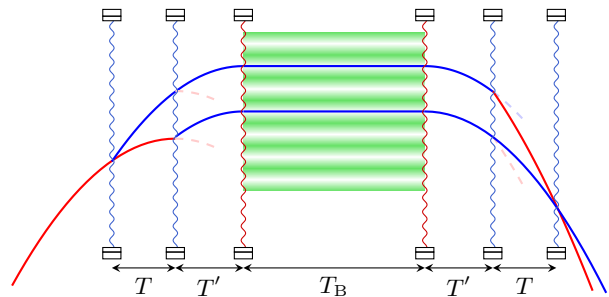


Figure 1. Proposed setup. All motion is restricted to one dimension (parallel to the gravitational field). Blue wavy lines represent  $\pi/2$  Bragg pulses splitting the trajectory of the atom, while red wavy lines represent the  $\pi/2$  clock pulses affecting only the internal state of the atom. The optical lattice (green striped pattern) is turned on exactly when the blue trajectories reach their apex and off after time  $T_B$ . Shaded dashed lines represent trajectories lost within the interferometer.

When the relevant trajectories reach the apex, namely at time  $T + T' = (v_0 + \Delta v)/g$ , the optical lattice is switched on, and atoms perform Bloch oscillations. At switching on the lattice we introduce our modification — a clock pulse at frequency  $\omega$  that puts atoms in an equal superposition of the two internal states without affecting its momentum [54–56]. The optical lattice remains on for time  $T_B$ , after which the second clock pulse is applied and the lattice is switched off. The atoms fall freely for time  $T'$ , after which another pair of  $\pi/2$  Bragg pulses is applied to recombine the trajectory. At this stage, another two trajectories are lost — this is different than in experiments [18–22] where all the output ports are measured but only two interfere (a modification that we introduce for simplicity of the subsequent analysis).

In the end, one measures the probabilities  $P_g^{(j)}$  that the atoms are found in the ground state in the output trajectory  $j \in \{0, 1\}$ , with 0 and 1 corresponding to the red and blue trajectories in Fig. 1, respectively). Apart from the non-relativistic phase  $\Delta\phi$  between the upper and lower ground state trajectories (measured in typical interferometric experiments, e.g. [20]), there will be additional phases  $\delta_d$  and  $\delta_u$  acquired within the optical lattice by the excited state on the lower and upper trajectory, respectively, which can be measured with the proposed setup. The probability  $P_g^{(j)}$  is given by (see Appendix A for derivation)

$$P_g^{(j)} = \frac{1}{16} \left[ 1 - \cos\left(\frac{\delta_u + \delta_d}{2}\right) \cos\left(\frac{\delta_u - \delta_d}{2}\right) + (-1)^j \times \right. \\ \left. \times 2 \cos\left(\Delta\phi + \frac{\delta_u - \delta_d}{2}\right) \sin\left(\frac{\delta_d}{2}\right) \sin\left(\frac{\delta_u}{2}\right) \right]. \quad (1)$$

One can get rid of the  $\Delta\phi$ -dependence by calculating the total probability  $P_g = P_g^{(0)} + P_g^{(1)}$  of finding the atom in

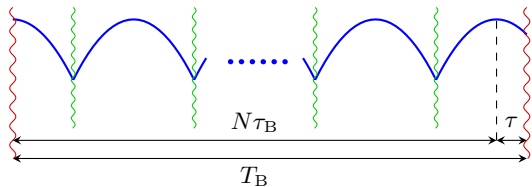


Figure 2. Trajectory followed by the atom (at the lower or upper trajectory) in the optical lattice. We adopt a simplified model of Bloch oscillations in which the atom follows a bouncing trajectory at a fixed height. The total time of Bloch oscillations  $T_B$  needs not be equal to an integer multiple of Bloch periods  $N\tau_B$ . Instead,  $T_B = N\tau_B + \tau$  with  $\tau \in (-\pi/2, \pi/2)$ .

the ground state

$$P_g = \frac{1}{8} \left[ 1 - \cos\left(\frac{\delta_u - \delta_d}{2}\right) \cos\left(\frac{\delta_u + \delta_d}{2}\right) \right]. \quad (2)$$

This probability does not depend on the specific opening and closure of the interferometer, but only on the part confined in the optical lattice. This part is central to our considerations because the atom will effectively behave as a clock at a superposition of heights within the optical lattice. The presence of two clock pulses is the main modification to previous experimental implementations [18–22]. Let us notice, that without those pulses, the probability of measuring the atoms in the ground state would be constant and equal to 1/4 (recall that we lose some of the trajectories). In our setup, they oscillate between 0 and 1/4, depending on the time  $T_B$  of the lattice hold.

—*Dynamics and phases.* Let us analyze the optical lattice stage of the interferometer and the additional phases  $\delta_d$  and  $\delta_u$  acquired by the excited state. At this stage, the atom will Bloch oscillate at a superposition of heights separated by  $\Delta z$ . We adopt a simplified model of Bloch oscillations (see [19, 57] and Fig. 2), in which the atom interacts with the optical lattice only when it reaches a downward velocity  $v_B = \hbar k/m$  (here  $k$  is the wave vector of the optical-lattice laser and  $m$  is the mass of the ground-state atom). Then, it instantaneously exchanges two photons with the lattice and changes its velocity. For the appropriately chosen frequency of the lattice light, the velocity at the interaction point will simply flip its sign, and the atom will oscillate at the fixed height with period  $\tau_B = 2v_B/g$ . We will assume that the laser frequency has been chosen exactly this way. Each bounce starts and ends at the apex of a free-fall trajectory. Within the time  $T_B$  the atom performs  $N$  oscillations with the last one possibly extended (or shortened) by a time  $\tau \in (-\tau_B/2, \tau_B/2)$  (this is because  $T_B$  is not necessarily an integer multiple of the Bloch period  $\tau_B$ ; see Fig. 2).

Crucially, due to the mass difference between the excited and the ground state of the atom, the condition for bouncing at the fixed height can be satisfied only for one of the internal states for a given lattice. For instance, if

we choose the lattice laser frequency so that the condition is satisfied for the ground state, the excited state will necessarily fall beyond the starting height with each oscillation. However, it can be shown (see Appendix B) that in viable experimental scenarios, the total fall is much smaller than the thermal wavelength of the atom. Therefore, employing the perturbative approach developed in [58] is justified, which here means that we can approximate that both the ground and the excited state follow the same trajectory. We further verify that this approximation holds in Appendix D.

The phases  $\delta_d$  and  $\delta_u$  consist of two components: laser phase  $\omega T_B$  acquired by the excited state due to the clock pulses, and a propagation phase correction due to different masses of the ground and the excited state. To calculate the latter we follow [58] and express the Lagrangian of the excited state  $L_e = L_g + \delta L$  in terms of the Lagrangian  $L_g$  of the ground state and a small correction  $\delta L$  resulting from the rest-mass difference between the ground and the excited state. If we denote this mass difference by  $\delta m = \hbar\omega_0/c^2$ , the Lagrangian correction is given by

$$\delta L = -\delta m (c^2 + gz - v^2/2). \quad (3)$$

Then, to calculate the propagation phase correction we integrate  $\delta L$  over the trajectory followed by the atom and divide by  $\hbar$ . The full calculation is presented in the Appendix C (followed by a non-perturbative calculation in Appendix D). It leads to the following formulae for the phases  $\delta_d$  and  $\delta_u$ :

$$\begin{aligned} \delta_d &= \left[ \omega - \omega_0 \left( 1 + \frac{\langle v^2 \rangle}{2c^2} \right) \right] T_B, \\ \delta_u &= \left[ \omega - \omega_0 \left( 1 + \frac{\langle v^2 \rangle}{2c^2} + \frac{g\Delta z}{c^2} \right) \right] T_B, \end{aligned} \quad (4)$$

where  $\langle v^2 \rangle = v_B^2/3$  is the mean square speed within a single oscillation.

In principle, the mass-energy corrections to the interferometric phases are not the only corrections of the order of  $1/c^2$  that are present in the proposed experiment — following [59] we could also include corrections coming from the higher-order expansion of the free-fall Lagrangian of the relativistic particle, and  $1/c^2$  corrections to the laser phases coming from elastic interactions (Bragg and Bloch pulses). These depend only on the trajectory followed by the atom and thus, in the picture in which ground and excited states follow the same trajectories, affect only the interferometric phase  $\Delta\phi$  leaving  $\delta_k$  and  $\delta_g$  unmodified. However, the  $1/c^2$  corrections to  $\Delta\phi$  are not the main focus of our considerations and we will not deal with them.

On the contrary, any corrections to the clock-pulse laser phases would affect  $\delta_k$  and  $\delta_g$  if they were present. Let us notice, however, that the corrections to the laser phases calculated in [59] resulted from the assumption that the atom-light interactions are always resonant and the atom interacts with photons with laboratory-frame

frequencies depending on its position and velocity. For our present purposes, we assume instead that the laser frequency of the clock pulses is fixed and the non-resonant processes are possible. Then, there are no corrections to the clock-pulse laser phases because the atom interacts with photons with the same laboratory-frame frequency regardless of its height and velocity.

—*Results and discussion.* Let us denote  $\varepsilon_k = \langle v^2 \rangle / 2c^2$  for the kinetic correction in Eq. (4) and  $\varepsilon_g = g\Delta z / c^2$  for the gravitational correction, and denote by  $\langle \omega_0 \rangle = \omega_0 (1 + \varepsilon_k + \varepsilon_g / 2)$  the (quantum mechanical) mean of the atomic internal frequency. Then, the probability of detecting the atom in the ground state (compare with Eq. (2)) can be written as

$$P_g = \frac{1}{8} [1 - \mathcal{V}(T_B) \cos([\omega - \langle \omega_0 \rangle] T_B)], \quad (5)$$

where  $\mathcal{V}(T_B) := \cos(\varepsilon_g \omega_0 T_B / 2)$  is the interferometric visibility. In a generic situation (away from the resonance), the visibility varies very slowly with time  $T_B$  compared to  $\cos([\omega - \langle \omega_0 \rangle] T_B)$ . Therefore, Eq. (5) describes an interference pattern with a slowly varying envelope. Apart from the visibility modulations, Eq. (5) looks like a result of a Ramsey interferometry experiment for an atom with internal transition frequency  $\langle \omega_0 \rangle$ . For fixed time  $T_B$  one can scan through different clock pulse frequencies  $\omega$  to find this resonant frequency. Thus, the relativistic effects coming from mass-energy equivalence can be measured in two ways: by observing the visibility oscillations, and by measuring the fractional frequency shift

$$\left\langle \frac{\delta \omega_0}{\omega_0} \right\rangle \equiv \frac{\langle \omega_0 \rangle - \omega_0}{\omega_0} = \varepsilon_k + \frac{\varepsilon_g}{2}. \quad (6)$$

Note that while the visibility oscillations are sensitive only to the gravitational correction  $\varepsilon_g$ , the frequency shift depends both on  $\varepsilon_g$  and  $\varepsilon_k$ . To distinguish between the gravitational and the kinetic effect in fractional frequency shift measurements, one can modulate the separation  $\Delta z$  between the upper and the lower trajectory — this will affect the gravitational correction, but not the kinetic one. The probability  $P_g$  as a function of time is visualized in Fig. 3 for exemplary values of  $\omega$ ,  $\omega_0$ ,  $\varepsilon_g$ , and  $\varepsilon_k$ .

Assuming the experimental parameters as in [20], we would have the velocity  $v_B \sim 10$  mm/s, and the vertical separation of the trajectories  $\Delta z \sim 10$   $\mu$ m. This would mean that the corrections would be of the order  $\varepsilon_k \sim \varepsilon_g \sim 10^{-22}$ . The fractional frequency shift of that order is very close to what can be currently detected [51, 52, 60, 61]. Indeed, state-of-the-art atomic clocks reach the multiple-measurement precision of the order of  $10^{-21}$  [51, 52, 61] (the single-measurement precision in these experiments is  $\sim 10^{-19}$ ), which is the order of magnitude for the fractional frequency shift in the proposed experiment for separations  $\Delta z \sim 100$   $\mu$ m, which has already been achieved in [20], at the expense of shorter coherence time.

On the other hand, for the transition frequency  $\omega_0 \sim 10^{15}$  Hz and lattice hold time  $T_B \sim 1$  s (numbers taken

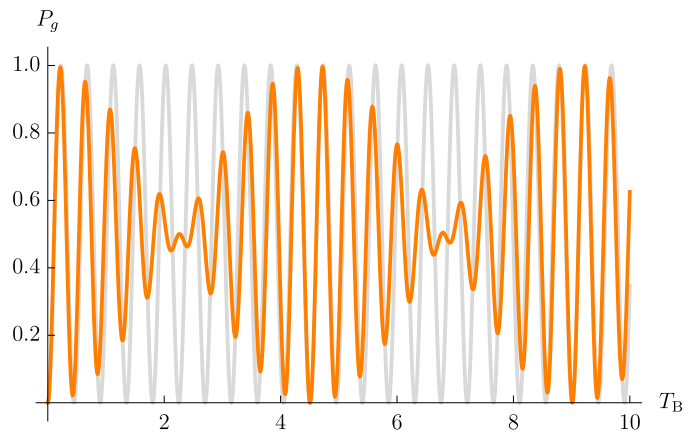


Figure 3. Oscillations of the (normalized) probability  $P_g$  for exemplary values  $\omega = 40\pi$ ,  $\omega_0 = 1.1\omega$ , and  $\varepsilon_k = 0.01$ , and two different values of the gravitational correction:  $\varepsilon_g = 0$  (in gray) and  $\varepsilon_g = \varepsilon_k$  (in orange). Note that, apart from visibility modulations, the orange pattern has its frequency shifted against the gray one.

from [20]), and  $\varepsilon_g \sim 10^{-22}$ , the visibility drop would be of the order of  $10^{-15}$ , which is certainly far beyond what can be currently observed in experiment. In principle, the properties of strontium atoms allow for keeping coherent Bloch oscillations for over 100 s [62]. While, to the best of our knowledge, the 1 s is the longest that has been achieved for strontium atoms so far, experiments with minute-scale oscillation times have been performed using cesium atoms [21, 22] (with these atoms, however, the frequency  $\omega_0$  is much smaller, so the effect would be even weaker). Extending the oscillation time to 100 s would enhance the visibility oscillations by  $10^4$ , but the effect would still be tiny. We expect that to make it observable, one would need to maintain a superposition separated by  $\Delta z \sim 10 - 100$  cm for 100 s — then the visibility drop would be of the order 0.01 – 1. Such separations are, however, far from what can be currently achieved and most likely require using two separate lasers for the lower and upper trajectories.

Note that the observation of the frequency shift (6) itself would not be evidence of the quantum clock reading the superposition of proper times since the frequency shift is the same as for the clock being in a statistical mixture of two heights. To reject the latter possibility one can, apart from the total probability  $P_g$  of measuring the atom in the ground state at the output, extract from the measured data also the difference  $D_g \equiv P_g^{(0)} - P_g^{(1)}$  given by (compare with Eq. (1))

$$D_g = \frac{1}{8} \cos\left(\Delta\phi + \frac{\delta_u - \delta_d}{2}\right) \sin\left(\frac{\delta_d}{2}\right) \sin\left(\frac{\delta_u}{2}\right), \quad (7)$$

where  $\delta_d$  and  $\delta_u$  are given in Eq. (4), and  $\Delta\phi$  is given by (see Appendix C for derivation)

$$\Delta\phi = -\frac{mg\Delta z}{\hbar} (T + 2T' + \tau). \quad (8)$$

If the atom is in a superposition of heights,  $D_g$  will oscillate with time  $T_B$ . On the other hand, for the atom following a statistical mixture of two heights, the probability difference would be equal to zero. Therefore, extracting from the interferometric output the fractional frequency shift and the oscillations of  $D_g$  would provide evidence that the atom was reading a superposition of proper times.

It is important to emphasize that the method proposed in this work does not rely on the assumption that ground and excited states follow the same trajectories within the optical lattice. While we showed that within the required order ( $1/c^2$ ) of calculating the phases acquired in the interferometer the trajectories associated with different mass-energy states can be approximated as equal, the method allows accounting for mass-energy corrections and resulting phases beyond this approximation.

Finally, let us notice that the interpretation of the experiment as a spectroscopy of a clock at the superposition of heights is possible thanks to including the

laser phases and the concrete mechanism that sets up the quantum clock. These were missing in the idealized scenarios in [23, 24] and in the recent work [38] proposing a similar setup using optical tweezers. Therefore, the possibility of measuring the relativistic frequency shift in such interferometric scenarios thus far went unnoticed.

## ACKNOWLEDGMENTS

We thank Timothy Le Pers, Navdeep Arya, Germain Tobar, and Jun Ye for helpful discussions and useful comments. The authors acknowledge Knut and Alice Wallenberg foundation through a Wallenberg Academy Fellowship No. 2021.0119. J.F. acknowledges funding from the U.S. Department of Energy, Office of Science, ASCR under Award Number DE-SC0023291 and Australian Research Council Centre of Excellence for Quantum Computation and Communication Technology (No. CE1701000012).

- 
- [1] A. Einstein, Zur elektrodynamik bewegter körper, *Annalen der physik* **4**, [10.1002/andp.19053221004](https://doi.org/10.1002/andp.19053221004) (1905).
  - [2] R. V. Pound and G. A. Rebka, Gravitational red-shift in nuclear resonance, *Phys. Rev. Lett.* **3**, 439 (1959).
  - [3] J. C. Hafele and R. E. Keating, Around-the-world atomic clocks: Predicted relativistic time gains, *Science* **177**, 166 (1972).
  - [4] I. I. Shapiro, Fourth test of general relativity, *Phys. Rev. Lett.* **13**, 789 (1964).
  - [5] I. I. Shapiro, M. E. Ash, R. P. Ingalls, W. B. Smith, D. B. Campbell, R. B. Dyce, R. F. Jurgens, and G. H. Pettengill, Fourth test of general relativity: New radar result, *Phys. Rev. Lett.* **26**, 1132 (1971).
  - [6] R. Colella, A. W. Overhauser, and S. A. Werner, Observation of gravitationally induced quantum interference, *Phys. Rev. Lett.* **34**, 1472 (1975).
  - [7] M. Kasevich and S. Chu, Atomic interferometry using stimulated Raman transitions, *Phys. Rev. Lett.* **67**, 181 (1991).
  - [8] M. Kasevich and S. Chu, Measurement of the gravitational acceleration of an atom with a light-pulse atom interferometer, *Applied Physics B* **54**, 321 (1992).
  - [9] A. Peters, K. Y. Chung, and S. Chu, Measurement of gravitational acceleration by dropping atoms, *Nature* **400**, 849 (1999).
  - [10] J. M. McGuirk, G. T. Foster, J. B. Fixler, M. J. Snadden, and M. A. Kasevich, Sensitive absolute-gravity gradiometry using atom interferometry, *Phys. Rev. A* **65**, 033608 (2002).
  - [11] J. B. Fixler, G. T. Foster, J. M. McGuirk, and M. A. Kasevich, Atom interferometer measurement of the Newtonian constant of gravity, *Science* **315**, 74 (2007).
  - [12] G. Lamporesi, A. Bertoldi, L. Cacciapuoti, M. Prevedelli, and G. M. Tino, Determination of the Newtonian gravitational constant using atom interferometry, *Phys. Rev. Lett.* **100**, 050801 (2008).
  - [13] G. Rosi, F. Sorrentino, L. Cacciapuoti, M. Prevedelli, and G. M. Tino, Precision measurement of the Newtonian gravitational constant using cold atoms, *Nature* **510**, 518 (2014).
  - [14] G. Rosi, L. Cacciapuoti, F. Sorrentino, M. Menchetti, M. Prevedelli, and G. M. Tino, Measurement of the gravity-field curvature by atom interferometry, *Phys. Rev. Lett.* **114**, 013001 (2015).
  - [15] T. Kovachy, P. Asenbaum, C. Overstreet, C. A. Donnelly, S. M. Dickerson, A. Sugarbaker, J. M. Hogan, and M. A. Kasevich, Quantum superposition at the half-metre scale, *Nature* **528**, 530 (2015).
  - [16] L. Hu, N. Poli, L. Salvi, and G. M. Tino, Atom interferometry with the Sr optical clock transition, *Phys. Rev. Lett.* **119**, 263601 (2017).
  - [17] P. Asenbaum, C. Overstreet, M. Kim, J. Curti, and M. A. Kasevich, Atom-interferometric test of the equivalence principle at the  $10^{-12}$  level, *Phys. Rev. Lett.* **125**, 191101 (2020).
  - [18] R. Charrière, M. Cadoret, N. Zahzam, Y. Bidet, and A. Bresson, Local gravity measurement with the combination of atom interferometry and Bloch oscillations, *Phys. Rev. A* **85**, 013639 (2012).
  - [19] M. Andia, R. Jannin, F. m. c. Nez, F. m. c. Biraben, S. Guellati-Khélifa, and P. Cladé, Compact atomic gravimeter based on a pulsed and accelerated optical lattice, *Phys. Rev. A* **88**, 031605 (2013).
  - [20] X. Zhang, R. P. del Aguila, T. Mazzoni, N. Poli, and G. M. Tino, Trapped-atom interferometer with ultracold Sr atoms, *Phys. Rev. A* **94**, 043608 (2016).
  - [21] V. Xu, M. Jaffe, C. D. Panda, S. L. Kristensen, L. W. Clark, and H. Müller, Probing gravity by holding atoms for 20 seconds, *Science* **366**, 745 (2019).
  - [22] C. D. Panda, M. Tao, J. Egelhoff, M. Ceja, V. Xu, and H. Müller, Coherence limits in lattice atom interferometry at the one-minute scale, *Nature Physics* [10.1038/s41567-024-02518-9](https://doi.org/10.1038/s41567-024-02518-9) (2024).
  - [23] S. Sinha and J. Samuel, Atom interferometry and the

- gravitational redshift, *Classical and Quantum Gravity* **28**, 145018 (2011).
- [24] M. Zych, F. Costa, I. Pikovski, and Č. Brukner, Quantum interferometric visibility as a witness of general relativistic proper time, *Nature Communications* **2**, 10.1038/ncomms1498 (2011).
- [25] M. Zych, F. Costa, I. Pikovski, T. C. Ralph, and Časlav Brukner, General relativistic effects in quantum interference of photons, *Classical and Quantum Gravity* **29**, 224010 (2012).
- [26] E. Castro Ruiz, F. Giacomini, and Č. Brukner, Entanglement of quantum clocks through gravity, *Proceedings of the National Academy of Sciences* **114**, E2303 (2017).
- [27] S. Loriani *et al.*, Interference of clocks: A quantum twin paradox, *Sci. Adv.* **5**, eaax8966 (2019).
- [28] A. Roura, Gravitational redshift in quantum-clock interferometry, *Phys. Rev. X* **10**, 021014 (2020).
- [29] E. Castro-Ruiz, F. Giacomini, A. Belenchia, and Č. Brukner, Quantum clocks and the temporal localisability of events in the presence of gravitating quantum systems, *Nat Commun* **11**, 2672 (2020).
- [30] A. R. H. Smith and M. Ahmadi, Quantum clocks observe classical and quantum time dilation, *Nat. Commun.* **11**, 5360 (2020).
- [31] S. Khandelwal, M. P. E. Lock, and M. P. Woods, Universal quantum modifications to general relativistic time dilation in delocalised clocks, *Quantum* **4**, 309 (2020).
- [32] P. T. Grochowski, A. R. H. Smith, A. Dragan, and K. Dębski, Quantum time dilation in atomic spectra, *Phys. Rev. Res.* **3**, 023053 (2021).
- [33] J. Paczos, K. Dębski, P. T. Grochowski, A. R. H. Smith, and A. Dragan, Quantum time dilation in a gravitational field, *Quantum* **8**, 1338 (2024).
- [34] K. Dębski, P. T. Grochowski, R. Demkowicz-Dobrzański, and A. Dragan, Universality of quantum time dilation, *Classical and Quantum Gravity* **41**, 135014 (2024).
- [35] P. A. Bushev, J. H. Cole, D. Sholokhov, N. Kukharchyk, and M. Zych, Single electron relativistic clock interferometer, *New Journal of Physics* **18**, 093050 (2016).
- [36] A. Roura, C. Schubert, D. Schlippert, and E. M. Rasel, Measuring gravitational time dilation with delocalized quantum superpositions, *Phys. Rev. D* **104**, 084001 (2021).
- [37] C. Ufrecht, F. Di Pumpo, A. Friedrich, A. Roura, C. Schubert, D. Schlippert, E. M. Rasel, W. P. Schleich, and E. Giese, Atom-interferometric test of the universality of gravitational redshift and free fall, *Phys. Rev. Res.* **2**, 043240 (2020).
- [38] I. Meltzer and Y. Sagi, Atomic clock interferometry using optical tweezers (2024), [arXiv:2402.14412 \[quant-ph\]](https://arxiv.org/abs/2402.14412).
- [39] M. Sonnleitner and S. M. Barnett, Mass-energy and anomalous friction in quantum optics, *Phys. Rev. A* **98**, 042106 (2018).
- [40] M. Zych, L. Rudnicki, and I. Pikovski, Gravitational mass of composite systems, *Phys. Rev. D* **99**, 104029 (2019).
- [41] P. K. Schwartz and D. Giulini, Post-Newtonian corrections to Schrödinger equations in gravitational fields, *Classical and Quantum Gravity* **36**, 095016 (2019).
- [42] P. K. Schwartz and D. Giulini, Post-Newtonian Hamiltonian description of an atom in a weak gravitational field, *Phys. Rev. A* **100**, 052116 (2019).
- [43] M. Zych, *Quantum Systems under Gravitational Time Dilation* (Springer Cham, 2017).
- [44] M. Zych and Č. Brukner, Quantum formulation of the Einstein equivalence principle, *Nature Physics* **14**, 1027 (2018).
- [45] F. Di Pumpo, C. Ufrecht, A. Friedrich, E. Giese, W. P. Schleich, and W. G. Unruh, Gravitational redshift tests with atomic clocks and atom interferometers, *PRX Quantum* **2**, 040333 (2021).
- [46] D. E. Krause and I. Lee, Taking einstein seriously: Relativistic coupling of internal and center of mass dynamics, *Eur. J. Phys.* **38**, 045401 (2017).
- [47] V. Yudin and A. Taichenachev, Mass defect effects in atomic clocks, *Laser Physics Letters* **15**, 035703 (2018).
- [48] R. Haustein, G. J. Milburn, and M. Zych, Mass-energy equivalence in harmonically trapped particles (2019), [arXiv:1906.03980 \[quant-ph\]](https://arxiv.org/abs/1906.03980).
- [49] V. J. Martínez-Lahuerta, S. Eilers, T. E. Mehlstäubler, P. O. Schmidt, and K. Hammerer, Ab initio quantum theory of mass defect and time dilation in trapped-ion optical clocks, *Phys. Rev. A* **106**, 032803 (2022).
- [50] A. Chu, V. J. Martínez-Lahuerta, M. Miklos, K. Kim, P. Zoller, K. Hammerer, J. Ye, and A. M. Rey, Exploring the interplay between mass-energy equivalence, interactions and entanglement in an optical lattice clock (2024), [arXiv:2406.03804](https://arxiv.org/abs/2406.03804).
- [51] T. Bothwell *et al.*, Resolving the gravitational redshift across a millimetre-scale atomic sample, *Nature* **602**, 420 (2022).
- [52] X. Zheng, J. Dolde, V. Lochab, B. N. Merriman, H. Li, and S. Kolkowitz, Differential clock comparisons with a multiplexed optical lattice clock, *Nature* **602**, 425 (2022).
- [53] In experiments [20–22] the temperature reaches a few hundreds of nanokelvins.
- [54] G. Grynberg, Remarks on E1-E2 and E1-M1 two-photon transitions, *Journal de Physique* **44**, 679 (1983).
- [55] E. A. Alden, K. R. Moore, and A. E. Leanhardt, Two-photon E1-M1 optical clock, *Phys. Rev. A* **90**, 012523 (2014).
- [56] G. Janson, A. Friedrich, and R. Lopp, Finite pulse-time effects in long-baseline quantum clock interferometry, *AVS Quantum Science* **6**, 10.1116/5.0178230 (2024).
- [57] M. Cadoret *et al.*, Atom interferometry based on light pulses: Application to the high precision measurement of the ratio  $h/m$  and the determination of the fine structure constant, *Eur. Phys. J. Spec. Top.* **172**, 121 (2009).
- [58] P. Storey and C. Cohen-Tannoudji, The Feynman path integral approach to atomic interferometry. A tutorial, *J. Phys. II France* **4**, 1999 (1994).
- [59] M. Werner, P. K. Schwartz, J.-N. Kirsten-Siemß, N. Gaaloul, D. Giulini, and K. Hammerer, Atom interferometers in weakly curved spacetimes using Bragg diffraction and Bloch oscillations, *Phys. Rev. D* **109**, 022008 (2024).
- [60] R. B. Hutson, A. Goban, G. E. Marti, L. Sonderhouse, C. Sanner, and J. Ye, Engineering quantum states of matter for atomic clocks in shallow optical lattices, *Phys. Rev. Lett.* **123**, 123401 (2019).
- [61] X. Zheng, J. Dolde, M. C. Cambria, H. M. Lim, and S. Kolkowitz, A lab-based test of the gravitational redshift with a miniature clock network, *Nat. Commun.* **14**, 4886 (2023).
- [62] M. G. Tarallo, A. Alberti, N. Poli, M. L. Chiofalo, F.-Y. Wang, and G. M. Tino, Delocalization-enhanced Bloch oscillations and driven resonant tunneling in optical lattices for precision force measurements, *Phys. Rev. A* **86**,

### Appendix A: Probability calculation

Here we derive the formula (1) for the probability  $P_g^{(j)}$  of measuring the atom in the ground state in output  $j \in \{0, 1\}$ . We denote by  $\Delta\phi$  the phase difference between upper and lower ground state trajectories, and by  $\delta_d$  and  $\delta_u$  the additional phase acquired by the excited state on the lower and upper trajectory, respectively. The final state of the atom  $|\psi_{\text{final}}\rangle$  can be written in a generic way

$$|\psi_{\text{final}}\rangle = \frac{1}{8} |g\rangle (|0\rangle [1 - e^{i\delta_d} + e^{i\Delta\phi} (1 - e^{i\delta_u})] - i|1\rangle [1 - e^{i\delta_d} - e^{i\Delta\phi} (1 - e^{i\delta_u})]) + \dots, \quad (\text{A1})$$

where  $|0\rangle$  and  $|1\rangle$  are the states corresponding to two relevant output trajectories, and dots at the end stand for the parts of the state irrelevant to our considerations (lost trajectories and excited state). The factor  $1/8 = (1/\sqrt{2})^6$  in front comes from six laser pulses applied to the atom (four Bragg pulses and two clock pulses). The minus signs in the bracket multiplying  $|0\rangle$  result from the fact that excited state trajectories interacted with a laser two more times than the ground state trajectories (two clock pulses) — each interaction gives rise to the factor  $ie^{i\phi_l}$  multiplying the corresponding trajectory (here  $\phi_l$  is the so-called laser phase and we absorb it into phases  $\Delta\phi$ ,  $\delta_d$ , and  $\delta_u$ ). The factor  $-i$  multiplying  $|1\rangle$  reflects the fact that trajectories leaving the interferometer in output 1 interacted with the odd number of Bragg pulses (the lower trajectory interacted once, the upper one three times), while the ones leaving in output 0 interacted with the even number (two) of Bragg pulses. Finally, the additional minus sign in the bracket multiplying  $|1\rangle$  comes from the fact that, in the case of trajectories leaving in output 1, the upper trajectory interacted with two more Bragg pulses than the lower one.

The amplitude of finding the atom in the ground state in the output  $j$  is given by

$$\langle g, j | \psi_{\text{final}} \rangle \propto \frac{1}{8} [1 - e^{i\delta_d} + (-1)^j e^{i\Delta\phi} (1 - e^{i\delta_u})], \quad (\text{A2})$$

where we omitted the common phase factor  $-i$  present in the case of  $j = 1$ . To calculate the probability  $P_g^{(j)}$  we take the absolute value squared of the above amplitude and get

$$P_g^{(j)} = |\langle g, j | \psi_{\text{final}} \rangle|^2 = \frac{1}{16} \left[ 1 - \cos\left(\frac{\delta_u + \delta_d}{2}\right) \cos\left(\frac{\delta_u - \delta_d}{2}\right) + (-1)^j 2 \cos\left(\Delta\phi + \frac{\delta_u - \delta_d}{2}\right) \sin\left(\frac{\delta_d}{2}\right) \sin\left(\frac{\delta_u}{2}\right) \right], \quad (\text{A3})$$

which is exactly Eq. (1).

### Appendix B: Fall of the excited-state trajectory

Let us motivate the use of the perturbative method [58] by analyzing the fall of the excited-state trajectory during Bloch oscillations. We assume that the frequencies of the optical lattice lasers are chosen such that the ground state follows a bouncing trajectory at a fixed height (i.e., each interaction with the laser occurs at the same height  $z_B$ ). Then, the excited-state trajectory necessarily falls with each bounce, due to its greater mass. Indeed, since we assume that the interaction with the laser occurs only when the atom reaches downward velocity  $v_B = \hbar k/m$ , and the momentum transferred to the atom in each interaction is the same for both the ground and the excited state, the excited state will move after each interaction with the upward velocity  $v_B - \delta v_B$ , where the velocity difference  $\delta v_B$  is given by

$$\delta v_B = 2v_B \frac{\delta m}{m}. \quad (\text{B1})$$

Since the velocity of the excited state right before each interaction is larger (in terms of the absolute value) than right after it, each subsequent interaction will occur lower by

$$\delta z_B = \frac{v_B \delta v_B}{g} \quad (\text{B2})$$

than the previous one meaning that the excited-state trajectory will progressively fall.

Also, the excited trajectory's smaller starting velocity means it will reach the downward velocity  $v_B$  faster than the ground state. Two subsequent interactions on the excited-state trajectory are separated by a time  $\tau_B - \delta\tau_B$ , where

$$\delta\tau_B = \frac{\delta v_B}{g}. \quad (\text{B3})$$

The spatial separation between the ground and the excited state trajectories is maximal when the excited state interacts with the laser. Then, it changes the direction of motion and meets the ground state trajectory at its interaction height  $z_B$ . Therefore, the trajectories meet repeatedly (at the interaction points of the ground state trajectory), but at each subsequent meeting point the excited-state trajectory has velocity lower by  $\delta v_B$  than at the previous meeting point (while the ground state moves there at velocity  $v_B$ ).

The largest separation between the  $n$ th and  $(n+1)$ th interaction on the ground state trajectory occurs at the moment of  $(n+1)$ th interaction on the excited-state trajectory and is equal to  $2n\delta z_B$ . For the experimental parameters from [20] (strontium atoms, optical lattice operating at 532 nm, around 500 oscillations) the maximal separation between the ground and excited state trajectories would be around  $10^{-13}$  m. This should be compared with the thermal wavelength of the atoms given by

$$\lambda_{\text{th}} = \sqrt{\frac{2\pi\hbar^2}{mk_B T}}, \quad (\text{B4})$$

where  $T$  is the temperature. In the experiment [20] the atoms were cooled to  $\sim 400$  nK, corresponding to  $\lambda_{\text{th}} \sim 10^{-7}$  m. Therefore, the thermal wavelength is much larger than the separation between the trajectories, and it is justified to use the perturbative approach in phase calculations.

### Appendix C: Phases

Let us calculate the phases  $\Delta\phi$ ,  $\delta_d$ , and  $\delta_u$  using the perturbative method developed in [58]. Each consists of two contributions: the propagation phase calculated by integrating the free-fall Lagrangian over the trajectory followed by the atom, and the laser phase resulting from atom-light interactions.

The free-fall Lagrangian of a relativistic particle with the internal two-level structure incorporating the mass-energy equivalence can be expanded to the order  $1/c^2$  as follows:

$$L = -\hat{m}c^2 - \hat{m} \left( gz - \frac{1}{2}v^2 \right) - \frac{\hat{m}}{c^2} \left( \frac{1}{2}g^2 z^2 - \frac{1}{8}v^4 + \frac{3}{2}gzv^2 \right) + \mathcal{O} \left( \frac{1}{c^4} \right). \quad (\text{C1})$$

Here  $\hat{m}$  is the mass operator returning  $m$  for the ground state, and  $m + \delta m$  (where  $\delta m = \hbar\omega_0/c^2$ ) for the excited state of the atom. At this point, we distinguish the  $1/c^2$  correction to the excited-state Lagrangian coming from the mass-energy equivalence

$$\delta L^{(1)} = -\delta m (gz - v^2/2), \quad (\text{C2})$$

and the correction to the (ground- and excited-state) Lagrangian coming from the expansion of the relativistic-particle Lagrangian up to  $1/c^2$  order

$$\delta L^{(2)} = -\frac{m}{c^2} \left( \frac{1}{2}g^2 z^2 - \frac{1}{8}v^4 + \frac{3}{2}gzv^2 \right). \quad (\text{C3})$$

Here we replaced  $\hat{m}$  by  $m$  because  $\delta m$  is of the order  $1/c^2$  and would contribute in higher order to the above expression. Note that for the scenario considered in this work, based on numbers from [20],  $\delta L^{(2)} \ll \delta L^{(1)}$ . This is because the internal energy of the atomic transition ( $\sim 1$  eV) is much larger than the kinetic energy of the atom or the gravitational energy difference between the trajectories (both  $\sim 10^{-10}$  eV).

Note also that the correction  $\delta L^{(2)}$  and the corrections to the laser phases derived in [59] depend only on the trajectory, not on the internal state. Therefore, in the picture in which both the ground and the excited state follow the same trajectory, they will contribute only to the phase  $\Delta\phi$ , not to  $\delta_d$  and  $\delta_u$ . We are not interested in  $1/c^2$  corrections to  $\Delta\phi$ , hence we will omit them in the subsequent analysis and focus only on the corrections coming from  $\delta L^{(1)}$ .

We begin with the calculation of  $\Delta\phi$ . To calculate the propagation phase contribution we divide the trajectory into freely falling pieces between points of interaction with the lasers and calculate the propagation phase by integrating the freely falling Lagrangian

$$L_g = -m (c^2 + gz - v^2/2) \quad (\text{C4})$$



along the trajectory. More precisely, for the free fall starting at time  $t_A$  and ending at  $t_B$ , the propagation phase is given by

$$\begin{aligned}\phi_p(t_A \rightarrow t_B) &= \frac{1}{\hbar} \int_{t_A}^{t_B} dt L_g = -\frac{m}{\hbar} \int_{t_A}^{t_B} dt (c^2 + gz - v^2/2) \\ &= -\frac{m}{\hbar} \left[ \left( c^2 + gz_A - \frac{1}{2} v_A^2 \right) (t_B - t_A) + v_A g (t_B - t_A)^2 - \frac{1}{3} g^2 (t_B - t_A)^3 \right],\end{aligned}\quad (\text{C5})$$

where  $z_A$  and  $v_A$  are the atom's position and velocity, respectively, at time  $t_A$ . Denote by  $t_j$  with  $j \in \{1, 2, 3, 4\}$  the times at which consecutive Bragg pulses are applied, and by  $t_i$  and  $t_f$  the times of the initial and final clock pulses, respectively. Notice that to match the notation from the main text, the times of application of particular pulses must satisfy

$$t_2 - t_1 = t_4 - t_3 = T, \quad t_i - t_2 = t_3 - t_f = T', \quad t_f - t_i = T_B. \quad (\text{C6})$$

Let us further denote the quantities corresponding to the lower and upper trajectories by superscripts (d) and (u), respectively, and by  $\Delta\phi_p(t_A \rightarrow t_B) = \phi_p^{(u)}(t_A \rightarrow t_B) - \phi_p^{(d)}(t_A \rightarrow t_B)$  the propagation phase difference between those two trajectories acquired between  $t_A$  and  $t_B$ . Let us consider one by one the consecutive stages of the interferometer and calculate the corresponding phase difference using (C5).

- $t_1 \rightarrow t_2$ :

At time  $t_1$  both trajectories are at the same height, but the upper one starts with a velocity greater by  $\Delta v$  than the lower one. Denote the initial velocity of the lower trajectory by  $v_1$ . Then, the relative propagation phase acquired between  $t_1$  and  $t_2$  reads

$$\Delta\phi_p(t_1 \rightarrow t_2) = \frac{m}{\hbar} \Delta v T \left( v_1 + \frac{1}{2} \Delta v - gT \right). \quad (\text{C7})$$

- $t_2 \rightarrow t_i$ :

Both trajectories start with the same velocity, but the upper one is higher by  $\Delta v T$ . The relative propagation phase is given by

$$\Delta\phi_p(t_2 \rightarrow t_i) = -\frac{m}{\hbar} g \Delta v T T'. \quad (\text{C8})$$

- $t_i \rightarrow t_f$ :

We assume that both trajectories oscillate with the same frequency, and start simultaneously with zero initial velocity and maximal height. Therefore, the trajectories are constantly separated by  $\Delta v T$  and have the same velocities all the time. The relative propagation phase equals

$$\Delta\phi_p(t_i \rightarrow t_f) = -\frac{m}{\hbar} g \Delta v T T_B. \quad (\text{C9})$$

- $t_f \rightarrow t_3$ :

Similar to the previous two points, the velocity on both trajectories is the same, and they are separated by  $\Delta v T$ . The propagation phase difference reads

$$\Delta\phi_p(t_f \rightarrow t_3) = -\frac{m}{\hbar} g \Delta v T T'. \quad (\text{C10})$$

- $t_3 \rightarrow t_4$ :

The trajectories start separated by  $\Delta v T$ , and the upper one has a velocity smaller by  $\Delta v$ . Denote the initial velocity of the lower trajectory by  $v_3$ . The relative propagation phase is then given by

$$\Delta\phi_p(t_3 \rightarrow t_4) = \frac{m}{\hbar} \Delta v T \left( -v_3 + \frac{1}{2} \Delta v \right). \quad (\text{C11})$$

To calculate the total propagation phase difference  $\Delta\phi_p$  we sum up all the contributions, which gives

$$\Delta\phi_p = \frac{m}{\hbar} \Delta v T [v_1 + \Delta v - v_3 - g(T + 2T' + T_B)]. \quad (\text{C12})$$

Finally, let us note that, because of the requirement that at  $t_i$  the velocity on both trajectories is equal to zero, the following relation holds

$$v_1 + \Delta v = g(T + T'). \quad (\text{C13})$$

On the other hand,  $v_3$  is the velocity that the atom reaches after time  $T'$  of a free fall after leaving the optical lattice. Let us notice that the atom does not leave the optical lattice with zero velocity (see Fig. 2), but rather with velocity  $-g\tau$ . Here  $\tau \in \{-\tau_B/2, \tau_B/2\}$  is given by

$$T_B = N\tau_B + \tau, \quad (\text{C14})$$

where  $N = \lfloor T_B/\tau_B + 1/2 \rfloor$  is the number of interactions between the optical lattice and the atom. Therefore, we have

$$v_3 = -g(\tau + T') \quad (\text{C15})$$

and we can rewrite Eq. (C12) (introducing  $\Delta z = \Delta v T$ ) as follows:

$$\Delta\phi_p = \frac{m}{\hbar} \Delta z g(\tau - T_B) = -\frac{m}{\hbar} g \Delta z N \tau_B. \quad (\text{C16})$$

Now, let us focus on the laser phase contribution to the phase  $\Delta\phi$ . As described in [58], when the atom absorbs (emits) a photon with frequency  $\omega$  and wave vector  $k$ , it acquires a laser phase

$$\phi_1(t, z) = \mp i\omega t \pm kz, \quad (\text{C17})$$

where the upper (lower) sign corresponds to photon absorption (emission), and  $t$  and  $z$  are the time and position of the interaction, respectively. In the case of Bragg pulses, as well as in the optical lattice, the photon absorption is immediately followed by the emission of a photon with the same frequency and opposite wave vector. Therefore, the laser phase acquired at each such interaction point is equal to  $\phi_1(t, z) = \phi_1(z) = \pm 2kz$  with the plus (minus) sign corresponding to the atom receiving upward (downward) momentum.

Denote by  $z_j$  with  $j \in \{1, 2, 3, 4\}$  the interaction heights with four consecutive Bragg pulses ( $z_1$  and  $z_3$  correspond to the upper trajectory, while  $z_2$  and  $z_4$  to the lower one), and by  $z_d$  and  $z_u$  the heights of interactions of the lower and upper trajectories, respectively, within the optical lattice. Note also that the wave vector  $k_{\text{Bragg}}$  of the pulses is related to the velocity change  $\Delta v$  by

$$2\hbar k_{\text{Bragg}} = m\Delta v, \quad \implies \quad k_{\text{Bragg}} = \frac{m\Delta v}{2\hbar}, \quad (\text{C18})$$

and the wave vector  $k_{\text{Bloch}}$  of the optical lattice laser is related to the Bloch period  $\tau_B$  by

$$2\hbar k_{\text{Bloch}} = mg\tau_B, \quad \implies \quad k_{\text{Bloch}} = \frac{mg\tau_B}{2\hbar}. \quad (\text{C19})$$

The total laser phase difference (between the upper and lower trajectory) is given by

$$\Delta\phi_1 = 2k_{\text{Bragg}}(z_1 - z_2 - z_3 + z_4) + 2Nk_{\text{Bloch}}(z_u - z_d) \quad (\text{C20})$$

Let us notice the following relations between particular heights:

$$z_2 - z_1 = v_1 T - \frac{1}{2}gT^2, \quad z_4 - z_3 = (v_3 - \Delta v)T - \frac{1}{2}gT^2, \quad z_u - z_d = \Delta z, \quad (\text{C21})$$

where  $v_1$  and  $v_3$  are given by (C13) and (C15). Hence, we can write the total laser phase difference as

$$\Delta\phi_1 = \frac{m}{\hbar} [-g\Delta z(T + 2T' + \tau) + g\Delta z N \tau_B]. \quad (\text{C22})$$

The total phase difference  $\Delta\phi$  between the upper and the lower (ground state) trajectories is calculated by summing up the total propagation phase difference and the total laser phase difference. This gives

$$\Delta\phi = \Delta\phi_p + \Delta\phi_1 = -\frac{mg\Delta z}{\hbar}(T + 2T' + \tau). \quad (\text{C23})$$

Now, let us calculate the additional phases  $\delta_d$  and  $\delta_u$  acquired by the excited state on the lower and upper trajectory, respectively. We need to calculate the additional laser phase coming from the clock pulses and the correction to the

propagation phase due to the mass-energy equivalence. Starting with the laser phase, we assume that the clock pulses change only the atom's internal state, but do not affect its motion. This can be achieved by driving two-photon transitions with both photons having the same frequency  $\omega/2$  and opposite momenta. The corresponding laser phase is equal to  $\mp\omega t$  with the minus (plus) sign corresponding to the two-photon absorption (emission). Note that this phase is independent of the position  $z$  of the interaction (thus, it is the same for the lower and upper trajectory). Since the excited state trajectories absorb the photons at  $t_i$  and emit at  $t_f$ , they acquire the laser phase  $\omega(t_f - t_i) = \omega T_B$ .

To calculate the propagation phase correction, we employ the perturbative method developed in [58] and integrate the mass-energy correction to the free-fall Lagrangian

$$\delta L = -\delta m (c^2 + gz - v^2/2) \quad (\text{C24})$$

over the ground state trajectory on the corresponding height. For the free-fall trajectory starting at  $t_A$  and ending at  $t_B$  the correction  $\delta_p(t_A \rightarrow t_B)$  to the propagation phase reads (compare with (C5))

$$\delta_p(t_A \rightarrow t_B) = -\frac{\delta m}{\hbar} \left[ \left( c^2 + gz_A - \frac{1}{2}v_A^2 \right) (t_B - t_A) + v_A g (t_B - t_A)^2 - \frac{1}{3}g^2 (t_B - t_A)^3 \right]. \quad (\text{C25})$$

For a full single oscillation in the optical lattice, the propagation phase correction  $\delta_{p,1}$  is given by

$$\delta_{p,1} = \frac{\delta m}{\hbar} \left( -c^2 - \frac{v_B^2}{6} - gz_B \right) \tau_B, \quad (\text{C26})$$

where  $z_B$  and  $v_B$  are the atom's position and velocity at the interaction point, and  $\tau_B$  is the period of the oscillation. We assume that the total number  $N$  of Bloch oscillations is large, and neglect the correction coming from the fact that the total time  $T_B$  of Bloch oscillations is not necessarily equal to the integer multiple of Bloch periods (instead,  $T_B = N\tau_B + \tau$  with  $\tau \in (-\tau_B/2, \tau_B/2)$ ); however, since  $\tau \ll N\tau_B$ , we will assume  $\tau \approx 0$ ). Then, the total propagation phase correction is given by

$$\delta_{p,\text{tot}} = N\delta_{p,1} = \frac{\delta m}{\hbar} \left( -c^2 - \frac{v_B^2}{6} - gz_B \right) N\tau_B \approx \frac{\delta m}{\hbar} \left( -c^2 - \frac{v_B^2}{6} - gz_B \right) T_B. \quad (\text{C27})$$

Without loss of generality, we can assume that the interaction height corresponding to the lower trajectory  $z_B^{(d)} = 0$ , while the interaction height of the upper one equals  $z_B^{(u)} = \Delta z$ . We introduce the mean velocity (within a single oscillation)  $\langle v^2 \rangle \equiv v_B^2/3$ , and note that  $\delta m = \omega_0/c^2$ . Combining the propagation phase with the laser phase corrections, we get

$$\begin{aligned} \delta_d &= \left[ \omega - \omega_0 \left( 1 + \frac{\langle v^2 \rangle}{2c^2} \right) \right] T_B, \\ \delta_u &= \left[ \omega - \omega_0 \left( 1 + \frac{\langle v^2 \rangle}{2c^2} + \frac{g\Delta z}{c^2} \right) \right] T_B. \end{aligned} \quad (\text{C28})$$

#### Appendix D: Non-perturbative calculations

As a consistency check let us compute the phases accumulated during the Bloch oscillations non-perturbatively, namely for the trajectories described in Appendix B, and make sure that they agree with the perturbative calculation from Appendix C. In the following, we restrict all the calculations to the terms up to order  $1/c^2$  neglecting the higher-order terms. This is consistent with the perturbative approach, where we considered only  $1/c^2$  corrections.

Since the trajectories of the ground and excited states no longer coincide (the excited trajectory falls), the phase difference between them will gain contribution from three different sources: the propagation phase, the laser phase, and the separation phase. The first two are defined in the same way as in the previous (perturbative) considerations, and the third one is given by

$$\delta_s(t) \equiv \frac{\bar{p}(t)\Delta z(t)}{\hbar}, \quad (\text{D1})$$

where  $\bar{p}(t)$  is the mean momentum of two trajectories at time  $t$  (the oscillation starts at  $t = 0$ ), and  $\Delta z(t)$  is the separation between them (note that this has nothing to do with the separation  $\Delta z$  between the upper and lower trajectory).

Since the phase acquired due to the interaction with the clock pulses is position-independent, it will not change in the non-perturbative analysis. Therefore, we consider only the phases acquired during the Bloch oscillations within the optical lattice. The trajectory followed by both trajectories has been described above. We analyze only the time between the two first interactions on the ground state trajectory (at some arbitrary height  $z_B$ ) and show that the phase difference between the ground and the excited state trajectories agrees with the perturbative calculations. It is straightforward that it will agree with the perturbative calculations also at later times.

The propagation phases acquired on both trajectories in the first part of the oscillation (before the second interaction of the excited state) can be calculated using the general formula for the propagation phase in free fall:

$$\phi_p^{(g/e)}(t) = \frac{m^{(g/e)}}{\hbar} \left[ \left( -c^2 + \frac{1}{2}v_0^2 - gz_0 \right) t - v_0gt^2 + \frac{1}{3}g^2t^3 \right], \quad (\text{D2})$$

(this is just Eq. (C5) with  $t_A \rightarrow 0$  and  $t_B \rightarrow t$ ) where  $m^{(g)} = m$  and  $m^{(e)} = m + \delta m$  are the masses of the atom in the ground and excited state, respectively,  $v_0$  is the initial velocity, and  $z_0$  is the initial height. For the ground state, we replace  $v_0$  by  $v_B$ , while for the excited state by  $v_B - \delta v_B$ . The initial height for both states is the same and equal to  $z_B$ .

The difference in propagation phases at time  $t$  is then given by

$$\delta_p(t) = \phi_p^{(e)}(t) - \phi_p^{(g)}(t) = \frac{\delta m}{\hbar} \left[ \left( -c^2 + \frac{1}{2}v_B^2 - gz_B \right) t - v_Bgt^2 + \frac{1}{3}g^2t^3 \right] - \frac{m}{\hbar}(v_B - gt)\delta v_Bt \quad (\text{D3})$$

(recall that we neglect the terms higher-order than  $1/c^2$ ). Let us notice that, since  $\delta v_Bt$  is just the separation  $\Delta z(t)$  between the trajectories, the second term in the above formula is equal in value but with the opposite sign to the separation phase

$$\delta_s(t) = \frac{\bar{p}(t)\delta v_Bt}{\hbar} = \frac{m}{\hbar}(v_B - gt)\delta v_Bt, \quad (\text{D4})$$

where  $\bar{p}(t) = m(v_B - gt) + \mathcal{O}(1/c^2)$ . Therefore, the total phase difference for  $t < \tau_B - \delta v_B/g$  is given by

$$\delta_p(t) + \delta_s(t) = \frac{\delta m}{\hbar} \left[ \left( -c^2 + \frac{1}{2}v_B^2 - gz_B \right) t - v_Bgt^2 + \frac{1}{3}g^2t^3 \right], \quad (\text{D5})$$

in agreement with the perturbative results (indeed, this is just the propagation phase correction calculated in the perturbative approach).

At the time  $\tau_B - \delta v_B/g$  the interaction of the atom on the excited trajectory with the laser occurs, and it acquires a laser phase

$$\phi_1^{(e)} = \frac{m}{\hbar}2v_B(z_B - \delta z_B) = \phi_1^{(g)} - \frac{m}{\hbar}\delta v_B\tau_B + \mathcal{O}(\delta m^2), \quad (\text{D6})$$

where  $\phi_1^{(g)}$  is the laser phase acquired by the ground state trajectory at time  $\tau_B$ . Let us notice that right before the second interaction of the excited state the separation phase is equal to

$$\delta_s(\tau_B - \Delta v/g - \varepsilon) = -\frac{m}{\hbar}v_B\delta v_Bt, \quad (\text{D7})$$

while right after the interaction it is  $\sim \mathcal{O}(1/c^4)$ , because the mean momentum is then  $\sim \mathcal{O}(1/c^2)$ . This situation (mean momentum  $\sim \mathcal{O}(1/c^2)$  and thus negligible value of separation phase) persists until the second interaction on the ground state trajectory, at which time both trajectories are at the same height, but the excited one has the velocity  $v_B - 2\delta v_B$ . At this point, we can repeat the whole analysis changing everywhere  $\delta v_B \rightarrow 2\delta v_B$ . Since the propagation phase difference acquired between the second interaction on the excited and on the ground trajectories is also  $\sim \mathcal{O}(\delta m^2)$ , the total phase difference after the first oscillation is equal to

$$\delta = \delta_p + \delta_s + \delta_l = \frac{\delta m}{\hbar} \left[ \left( -c^2 + \frac{1}{2}v_B^2 - gz_B \right) \tau_B - v_Bg\tau_B^2 + \frac{1}{3}g^2\tau_B^3 \right] = \frac{\delta m}{\hbar} \left( -c^2 - \frac{v_B^2}{6} - gz_B \right) \tau_B, \quad (\text{D8})$$

which is equal to the propagation phase correction calculated for a single oscillation in the perturbative approach (compare with Eq. (C26)).